

## One-Pot Synthesis of a New Magnetically Coupled Heterometallic $\text{Cu}_2\text{Mn}_2 [2 \times 2]$ Molecular Grid

Yurii S. Moroz,<sup>†</sup> Łukasz Szyrwił,<sup>‡</sup> Serhiy Demeshko,<sup>§</sup> Henryk Kozłowski,<sup>‡</sup> Franc Meyer,<sup>§</sup> and Igor O. Fritsky<sup>\*†</sup>

<sup>†</sup>Department of Chemistry, Kiev National Taras Shevchenko University, Volodymyrska Street 64, 01601 Kiev, Ukraine, <sup>‡</sup>Faculty of Chemistry, University of Wrocław, F. Joliot-Curie 14, 50-383 Wrocław, Poland, and <sup>§</sup>Institut für Anorganische Chemie, Georg-August-Universität Göttingen, Tammannstrasse 4, D-37077 Göttingen, Germany

Received March 24, 2010

The heterometallic  $[2 \times 2]$  grid-type complex  $[\text{Cu}_2\text{Mn}_2(\text{pop})_4(\text{OAc})_4] \cdot 7\text{H}_2\text{O}$  (**1**) has been selectively synthesized in a targeted one-pot reaction. Single-crystal X-ray analysis shows the expected structure with identical metal ions located at diagonal vertices of the grid. Magnetochemical studies reveal that **1** has a ferrimagnetic spin ground state with some admixture of low-lying excited states.

Molecular grid-type complexes attract considerable attention as an interesting class of compounds in the area of nanoscale materials.<sup>1</sup> Numerous  $[n \times n]$  and  $[n \times m]$  grids (where  $n$  and  $m = 2-5$ ) containing paramagnetic metal ions have been prepared to date that may exhibit interesting optical and magnetic properties including spin crossover.<sup>2-8</sup> Antiferromagnetic coupling has been observed in almost all cases except some  $\text{Cu}^{\text{II}}$ -containing  $[2 \times 2]$  molecular grids, where, because of the orthogonal arrangement of the  $d_{x^2-y^2}$  magnetic orbitals, ferromagnetic exchange interaction is realized.<sup>9-11</sup> An attractive strategy for the preparation of

“nonzero ground-state” grid complexes is the synthesis of heterometallic complexes that contain metals with different numbers of unpaired electrons, giving a ferrimagnetic situation. Previous efforts in this direction have resulted in the preparation of few mixed-metal exchange-coupled clusters such as  $\text{Ni}_2\text{Fe}_2$  or  $\text{Fe}_3\text{Cu}_1$ .<sup>12,13</sup> Some examples of heterometallic  $[2 \times 2]$  grids with diamagnetic metal ions have also been reported.<sup>14,15</sup> In almost all of these cases, a two-step synthetic procedure has been applied, either via mononuclear complexes in the first step or by use of ligands with easily eliminated blocking groups. Most compartmental ligands used in this respect are symmetrical or have two rather similar binding pockets. However, nonsymmetric ligand strands with two pockets of different donor strength can clearly simplify the synthetic procedure and lead to mixed-metal grid complexes directly.

This report describes the one-pot synthesis of a new  $\text{Cu}_2\text{Mn}_2 [2 \times 2]$  gridlike exchange-coupled cluster based on the easy-to-prepare nonsymmetric ligand strand 2-(hydroxyimino)- $N'$ -[1-(2-pyridyl)ethylidene]propanohydrazide (**Hpop**; Chart 1), which provides two distinct donor compartments: a tridentate  $\{\text{N}_2\text{O}\}$  site<sup>16</sup> and a bidentate  $\{\text{NO}\}$  site.

It was shown previously that **Hpop** is a good precursor for  $[2 \times 2]$  molecular grids that may feature supramolecular isomerism with respect to the disposition of tridentate and bidentate donor sets in the grids.<sup>11</sup> This prompted us to explore the possibility of obtaining mixed-metal complexes in a controlled way. The system  $2\text{Hpop} - \text{Cu}(\text{OAc})_2 - \text{Mn}(\text{OAc})_2 - 2\text{KOH}$  in a  $\text{MeOH}/\text{H}_2\text{O}$  solution was thus monitored by electrospray ionization mass spectrometry (ESI-MS). The most predominant pattern observed in the ESI-MS spectrum

\*To whom correspondence should be addressed. E-mail: ifritsky@univ.kiev.ua.

(1) Ruben, M.; Rojo, J.; Romero-Salguero, F. J.; Uppadine, L. H.; Lehn, J. M. *Angew. Chem., Int. Ed.* **2004**, *43*, 3644–3662.

(2) Dawe, L. N.; Shuvaev, K. V.; Thompson, L. K. *Chem. Soc. Rev.* **2009**, *38*, 2334–2359.

(3) Stadler, A. M. *Eur. J. Inorg. Chem.* **2009**, 4751–4770.

(4) Klingele, J.; Prikhod'ko, A. I.; Leibeling, G.; Demeshko, S.; Dechert, S.; Meyer, F. *Dalton Trans.* **2007**, 2003–2013.

(5) van der Vlugt, J. I.; Demeshko, S.; Dechert, S.; Meyer, F. *Inorg. Chem.* **2008**, *47*, 1576–1585.

(6) Breuning, E.; Ruben, M.; Lehn, J. M.; Renz, F.; Garcia, Y.; Ksenofontov, V.; Gutlich, P.; Wegelius, E.; Rissanen, K. *Angew. Chem., Int. Ed.* **2000**, *39*, 2504–2507.

(7) Ruben, M.; Breuning, E.; Lehn, J. M.; Ksenofontov, V.; Gutlich, P.; Vaughan, G. *J. Magn. Magn. Mater.* **2004**, *272*, E715–E717.

(8) Ruben, M.; Lehn, J. M.; Vaughan, G. *Chem. Commun.* **2003**, 1338–1339.

(9) Matthews, C. J.; Avery, K.; Xu, Z. Q.; Thompson, L. K.; Zhao, L.; Miller, D. O.; Biradha, K.; Poirier, K.; Zaworotko, M. J.; Wilson, C.; Goeta, A. E.; Howard, J. A. K. *Inorg. Chem.* **1999**, *38*, 5266–5276.

(10) Xu, Z. Q.; Thompson, L. K.; Miller, D. O. *J. Chem. Soc., Dalton Trans.* **2002**, 2462–2466.

(11) Moroz, Y. S.; Kulon, K.; Haukka, M.; Gumienna-Kontecka, E.; Kozłowski, H.; Meyer, F.; Fritsky, I. O. *Inorg. Chem.* **2008**, *47*, 5656–5665.

(12) Xu, Z. Q.; Thompson, L. K.; Matthews, C. J.; Miller, D. O.; Goeta, A. E.; Howard, J. A. K. *Inorg. Chem.* **2001**, *40*, 2446–2449.

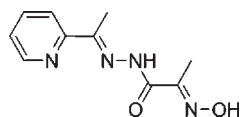
(13) Parsons, S. R.; Thompson, L. K.; Dey, S. K.; Wilson, C.; Howard, J. A. K. *Inorg. Chem.* **2006**, *45*, 8832–8834.

(14) Petitjean, A.; Kyritsakas, N.; Lehn, J. M. *Chem. Commun.* **2004**, 1168–1169.

(15) Bassani, D. M.; Lehn, J. M.; Serroni, S.; Puntoriero, F.; Campagna, S. *Chem.—Eur. J.* **2003**, *9*, 5936–5946.

(16) Manoj, E.; Kurup, M. R. P.; Fun, H. K.; Punnoose, A. *Polyhedron* **2007**, *26*, 4451–4462.

Chart 1. Structure of Hpop



could be assigned to the tetranuclear heterometallic species  $\{[\text{Cu}_2\text{Mn}_2(\text{pop})_4(\text{OAc})_4] + \text{K}\}^+$  ( $m/z$  1389.10; Figure S1 in the Supporting Information), while no signals corresponding to any homometallic polynuclear species were observed. This suggested that a simple one-pot reaction should directly lead to the  $\text{Cu}_2\text{Mn}_2 [2 \times 2]$  grid system as the preferred product, and indeed a mixture of  $\text{Cu}(\text{OAc})_2 \cdot 2\text{H}_2\text{O}$  (1 mmol) and  $\text{Mn}(\text{OAc})_2 \cdot 4\text{H}_2\text{O}$  (1 mmol) with Hpop (2 mmol) and KOH (2 mmol) in a MeOH/H<sub>2</sub>O solution afforded yellow-green single crystals of  $[\text{Cu}_2\text{Mn}_2(\text{pop})_4(\text{OAc})_4] \cdot 7\text{H}_2\text{O}$  (**1**) in 72% yield.

The complex molecule in **1** has the anticipated  $[2 \times 2]$  gridlike topology with two pairs of parallel ligand strands, as revealed by X-ray crystallography (Figure 1). The four metal ions are bridged by the hydrazone O atoms, with two of those bridging O atoms (O1 and O9) located above the  $\text{Cu}_2\text{Mn}_2$  mean plane and the two others (O5 and O13) located below it. This results in a boatlike overall arrangement (Figure S2 in the Supporting Information). Metal ions of the same kind are located at opposite vertices of the  $\text{M}_2\text{M}'_2$  tetragon.

The overall structure **1** is similar to that reported for homometallic  $[\text{Ni}_4(\text{pop})_4(\text{HCOO})_4] \cdot 7\text{H}_2\text{O}$ :<sup>11</sup> the pop ligand strands are oriented in a “head-to-head” arrangement at the  $\text{Cu}^{2+}$  sites and “tail-to-tail” when coordinated to  $\text{Mn}^{2+}$  (the terms “head” and “tail” refer to tridentate and bidentate donor pockets, respectively). Two different types of coordination polyhedra are thus realized in the grid:  $\text{Cu}\{\text{N}_4\text{O}_2\}$  and  $\text{Mn}\{\text{N}_2\text{O}_4\}$ . The former are best described as square-bipyramidal ( $[4 + 2]$ ) where axial positions of the  $\text{Cu}^{2+}$  ions are occupied by N5/N13 from the pyridine groups and O5/O13 from the hydrazone groups of the same pop ligands. Jahn–Teller axes of the  $\text{Cu}^{2+}$  polyhedra are almost parallel to each other [the dihedral angle between equatorial planes is  $15.6(2)^\circ$ ].  $\text{Mn}\{\text{N}_2\text{O}_4\}$  polyhedra are distorted octahedra formed by two N atoms belonging to the oxime groups, two O atoms from the hydrazone groups, and two O atoms from the coordinated exogenous acetate anions. All bond lengths (Table S1 in the Supporting Information) are in the usual range for six-coordinate  $\text{Cu}^{2+}$  and  $\text{Mn}^{2+}$  complexes with hydrazone and pyridine ligands.<sup>11,17</sup>

Each pop ligand forms three five-membered chelate rings. Additional seven-membered pseudochelate rings are found at the  $\text{Mn}\{\text{N}_2\text{O}_4\}$  polyhedra because of an intramolecular hydrogen bond between the oxime group and the nearby acetate O atom.  $\text{Cu} \cdots \text{Mn}$  separations between neighboring metal ions in the grid are very similar and close to 4 Å;  $\text{Cu}—\text{O}—\text{Mn}$  angles fall in the range  $133–135^\circ$ .

Selective formation of the heterometallic  $\text{Cu}_2\text{Mn}_2$  grid structure is probably favored for thermodynamic reasons. One may suggest that all possible mononuclear  $\text{Cu}^{2+}$  and  $\text{Mn}^{2+}$  1:2 species are initially formed in the reaction mixture, with different arrangements of Hpop around the central metal ions: “head-to-head”, “head-to-tail”, and “tail-to-tail”. The first type should be the most stable because each Hpop

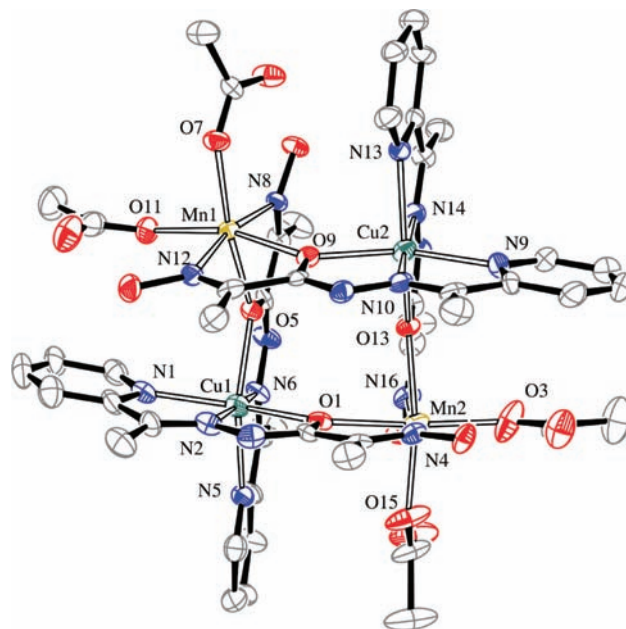


Figure 1. ORTEP-3 projection of the complex molecule in **1** (blue, N; red, O; gray, C). H atoms are omitted for clarity (40% probability thermal ellipsoids).

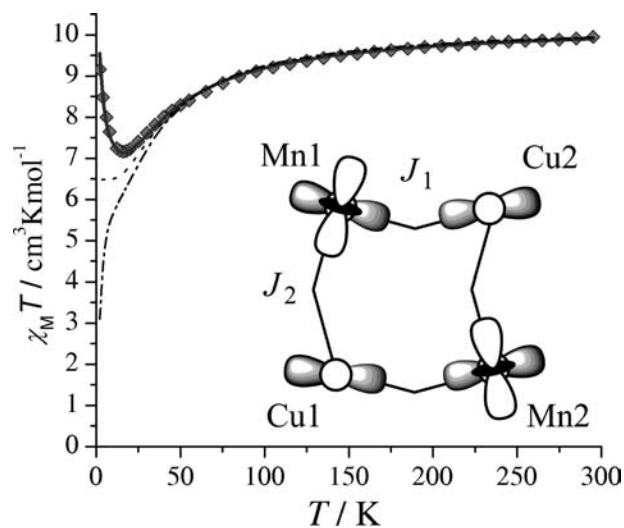


Figure 2. Magnetic data for **1**. The solid line represents the best curve fit (see the text), the dashed line shows a calculated curve for the “dimer-only” model ( $J_2 = 0$ ), and the dash-dotted line represents a  $J_2 > 0$  model. The inset shows a schematic drawing of the arrangement of  $\text{Mn}^{2+}$  and  $\text{Cu}^{2+}$  magnetic orbitals in **1**.

ligand forms two chelate rings. The stability of  $\text{Cu}^{2+}$ -containing “head-to-head” complexes is higher in comparison with  $\text{Mn}^{2+}$  species because of the crystal-field stabilization energy ( $+0.6\Delta_{\text{OCT}}$ ). Thus, one may assume that the  $\text{Cu}^{2+}$  “head-to-head” 1:2 complex is the primary building block that is then associated by  $\text{Mn}^{2+}$  ions in the final  $[2 \times 2]$  gridlike structure. A more detailed study of the mechanism of grid formation in these systems is in progress.

The magnetic properties of **1** are shown in Figure 2 as the temperature dependence of  $\chi_M T$ . The value of  $\chi_M T$  at room temperature is  $9.95 \text{ cm}^3 \text{ K mol}^{-1}$ , i.e., close to the spin-only value for two  $S = 5/2$   $\text{Mn}^{2+}$  and two  $S = 1/2$   $\text{Cu}^{2+}$  ions that are uncoupled ( $9.50 \text{ cm}^3 \text{ K mol}^{-1}$ ). The signature of the

(17) Matthews, C. J.; Thompson, L. K.; Parsons, S. R.; Xu, Z. Q.; Miller, D. O.; Heath, S. L. *Inorg. Chem.* **2001**, *40*, 4448–4454.

$\chi_M T$  vs  $T$  plot is typical for compounds with a ferrimagnetic ground state: intramolecular antiferromagnetic coupling causes  $\chi_M T$  to drop as the temperature is lowered, but the  $\chi_M T$  curve goes through a minimum at 12 K and rises at even lower temperatures. This characterizes a mixed-metal tetranuclear system with nonzero total spin (the expected  $\chi_M T$  value for an  $S_T = 4$  ground state is  $10.00 \text{ cm}^3 \text{ K mol}^{-1}$ ).<sup>18,19</sup> Experimental magnetic data for **1** were simulated based on the appropriate Hamiltonian for isotropic exchange and Zeeman splitting ( $S_1 = S_3 = 1/2$ ,  $S_2 = S_4 = 5/2$ ), which involves two parameters  $J_1$  (corresponding to magnetic coupling between Cu1–Mn2 and Cu2–Mn1) and  $J_2$  (coupling between Cu1–Mn1 and Cu2–Mn2).

$$\hat{H} = -2J_1(\hat{S}_1 \cdot \hat{S}_2 + \hat{S}_3 \cdot \hat{S}_4) - 2J_2(\hat{S}_2 \cdot \hat{S}_3 + \hat{S}_1 \cdot \hat{S}_4) + \sum_{i=1}^4 g_i \mu_B B \hat{S}_{iz}$$

The presence of two different exchange pathways is rationalized by the structural features and the resulting arrangement of the magnetic orbitals (inset in Figure 2). As described above, the elongated Jahn–Teller axes of Cu1 and Cu2 that represent the orientation of the nonmagnetic  $d_{z^2}$  orbitals can be identified along the N5···O5 and N13···O13 directions.

Exchange along this pathway ( $J_2$ ) is not very efficient but cannot be neglected because the arrangement of the magnetic  $d$  orbitals of  $\text{Cu}^{2+}$  and  $\text{Mn}^{2+}$  is not strictly orthogonal (the dihedral angles between {Cu1, O1, N1, N2, N6} and {Mn1, O9, O11, N8, N12} as well as {Cu2, O9, N9, N10, N14} and {Mn2, O1, O3, N4, N16} mean planes are  $16.7(2)^\circ$  and  $16.1(2)^\circ$ , respectively). This can be expected to result in some antiferromagnetic coupling along the  $J_2$  pathway. In contrast, exchange interaction between Mn1–Cu2 and Cu2–Mn1 is mediated via  $\sigma$  overlap of the magnetic  $d_{x^2-y^2}$  orbitals of  $\text{Cu}^{2+}$  with magnetic  $\text{Mn}^{2+}$  orbitals, which gives rise to a much stronger coupling ( $J_1$ ). In essence, the  $\text{Mn}_2\text{Cu}_2$  grid **1** can be viewed as a “dimer of dimers”.

Simulation of the experimental data<sup>20</sup> gave  $g_{\text{av}} = 2.08$ ,  $J_1 = -7.49 \text{ cm}^{-1}$ ,  $J_2 = -0.58 \text{ cm}^{-1}$ ,  $\text{TIP} = 0.65 \times 10^{-4} \text{ cm}^3 \text{ K mol}^{-1}$ ,  $\rho = 0.5\%$  ( $S = 2.5$ ) (TIP = temperature-independent paramagnetism;  $\rho$  = Curie-behaved paramagnetic monomer

impurities). The best fit is illustrated as the solid line in Figure 2. Simulations for a “dimer-only” model ( $J_2 = 0$ ) or assuming ferromagnetic exchange along the  $J_2$  pathway ( $J_2 = +0.58 \text{ cm}^{-1}$ ) does not properly reflect the experimental curve (dashed and dash-dotted lines in Figure 2).

Field-dependent magnetization studies have been carried out at 2 K and showed  $M$  rising steeply to a value of  $7.85 N\beta$  at 5 T (Figure S3 in the Supporting Information). Variable-field variable-temperature magnetization data do not show any significant zero-field splitting. Our efforts to fit the data using the appropriate Brillouin function led to  $g_{\text{av}} = 1.95$  and  $S = 4$  (2 K) when  $S$  was fixed or  $g_{\text{av}} = 2.07$  and  $S = 3.75$  (2 K) when  $g_{\text{ave}}$  was fixed. The latter  $S$  value is smaller than expected from a vector coupling scheme for the  $\text{Cu}_2\text{Mn}_2$  cluster with a ferrimagnetic ground state ( $S = 4$ ) because of the presence of unequal exchange pathways ( $|J_1| \gg |J_2|$ ) and may be a result of the mixing of ground and excited states with different multiplicities even at low values of the external magnetic field (Figure S4 in the Supporting Information).

In summary, the mixed-metal  $[2 \times 2]$  grid complex **1** has been selectively synthesized in a simple one-pot procedure. All structure-directing information is contained in the **pop** ligand that features two distinct sets of donor compartments, preset for the different metals. This illustrates a simple route for obtaining ferrimagnetic heterometallic grids with nonzero total spin, which may become useful precursors of novel molecular magnetic materials. **1** has the anticipated ferrimagnetic spin ground state with some admixture of low-lying excited states. The presence of exogenous labile acetate ligands as well as noncoordinating oxime O atoms adds another interesting aspect to these particular gridlike complexes because assembly of the  $\text{M}_2\text{M}'_2$  entities into high-nuclearity or two-dimensional extended compounds with  $[2 \times 2]$  gridlike building blocks may become possible via these sites. The recent isolation of a **pop**-based  $\text{Ni}_{12}$  complex that is composed of three  $[2 \times 2]$   $\text{Ni}_4$  subunits encourages further investigations in that direction.<sup>21</sup>

**Acknowledgment.** Financial support by the DFG (SFB 602, project A16) is gratefully acknowledged.

**Supporting Information Available:** Synthetic details, crystal data (CIF and structural data in Table S1), part of the ESI-MS spectrum (Figure S1), central fragment of the molecular structure (Figure S2), field-dependent magnetization measurements (Figure S3), and a section of the calculated energy level calculation scheme (Figure S4). This material is available free of charge via the Internet at <http://pubs.acs.org>.

(18) Li, D. F.; Parkin, S.; Wang, G. B.; Yee, G. T.; Holmes, S. M. *Inorg. Chem.* **2006**, *45*, 2773–2775.

(19) Karadas, F.; Schelter, E. J.; Shatruck, M.; Prosvirin, A. V.; Bacsa, J.; Smirnov, D.; Ozarowski, A.; Krzystek, J.; Telsler, J.; Dunbar, K. R. *Inorg. Chem.* **2008**, *47*, 2074–2082.

(20) Simulation of the experimental magnetic data was performed with the *julX* program (Bill, E., M.-P.-I. f. B. C.: Mülheim/Ruhr, Germany, [http://www.mpi-muelheim.mpg.de/bac/logins/bill/julX\\_en.php](http://www.mpi-muelheim.mpg.de/bac/logins/bill/julX_en.php)).

(21) Moroz, Y. S.; Demeshko, S.; Haukka, M.; Meyer, F.; Fritsky, I. O. Unpublished results.